Oncogenic transformation in the absence of Xrcc4 targets peripheral B cells that have undergone editing and switching

Jing H. Wang,[1,2,3,4] Frederick W. Alt,[1,2,3,4] Monica Gostissa,[1,2,3,4] Abhishek Datta,[1,2,3,4] Michael Murphy,[1,2,3,4] Marat B. Alimzhanov,[3] Kristen M. Coakley,[1,2,3,4] Klaus Rajewsky,[3,5] John P. Manis,[2,5] and Catherine T. Yan[1,2,3,4]

[1]Howard Hughes Medical Institute, [2]The Children's Hospital, [3]Immune Disease Institute, [4]Department of Genetics, [5]Department of Pathology, Harvard Medical School, MA 02115

Nonhomologous end-joining (NHEJ) repairs DNA double-strand breaks (DSBs) during V(D)J recombination in developing lymphocytes and during immunoglobulin (Ig) heavy chain (IgH) class switch recombination (CSR) in peripheral B lymphocytes. We now show that CD21-cre–mediated deletion of the *Xrcc4* NHEJ gene in p53-deficient peripheral B cells leads to recurrent surface Ig-negative B lymphomas ("CXP lymphomas"). Remarkably, CXP lymphomas arise from peripheral B cells that had attempted both receptor editing (secondary V[D]J recombination of Igκ and Igλ light chain genes) and *IgH* CSR subsequent to *Xrcc4* deletion. Correspondingly, CXP tumors frequently harbored a CSR-based reciprocal chromosomal translocation that fused *IgH* to *c-myc*, as well as large chromosomal deletions or translocations involving *Igκ* or *Igλ*, with the latter fusing *Igλ* to oncogenes or to *IgH*. Our findings reveal peripheral B cells that have undergone both editing and CSR and show them to be common progenitors of CXP tumors. Our studies also reveal developmental stage-specific mechanisms of *c-myc* activation via *IgH* locus translocations. Thus, Xrcc4/p53-deficient pro–B lymphomas routinely activate *c-myc* by gene amplification, whereas Xrcc4/p53-deficient peripheral B cell lymphomas routinely ectopically activate a single *c-myc* copy.

CORRESPONDENCE
Frederick W. Alt:
alt@enders.tch.harvard.edu

Abbreviations used: A-EJ, alternative end-joining; AID, activation-induced cytidine deaminase; C-NHEJ, classical NHEJ; CSR, class switch recombination; DSB, double-strand break; FISH, fluorescence in situ hybridization; NHEJ, nonhomologous end-joining; QM, quasimonoclonal; RS, recombination signal sequence; SHM, somatic hypermutation; SKY, spectral karyotyping.

Ig heavy (IgH) and light (IgL) chain variable region exons are assembled from component V, D, and J segments in developing B lymphocytes. V(D)J recombination is initiated by the RAG1/2 endonuclease, which introduces DNA double-strand breaks (DSBs) between V, D, and J segments and flanking recombination signal sequences (RSs) (1). Subsequently, cleaved coding segments are joined to form V(D)J exons and RSs are joined to form RS joins (2). Both coding and RS joining are performed by classical nonhomologous end-joining (C-NHEJ), which is a major general DSB repair pathway in mammalian cells (3). Xrcc4 and DNA Ligase IV (Lig4) form a complex that is required for V(D)J recombination (4, 5). In their absence, coding or RS ends are joined at low frequency, usually with substantial sequence deletion from one or both partners (6, 7). In mice, *Xrcc4* inactivation results in severe combined immune deficiency owing to inability to complete V(D)J recombination (6).

In progenitor B (pro–B) cells in the mouse BM, productive assembly of variable region exons within the IgH locus (*Igh*) on chromosome 12 leads to production of IgH μ chains that signal differentiation to the precursor B (pre–B) cell stage in which IgL variable region exons are assembled (8). Mice, like humans, have two IgL families, termed Igκ and Igλ, which are encoded by *Igκ* and *Igλ* loci that, respectively, lie on chromosomes 6 and 16. Igκ and Igλ expression is "isotype" excluded, such that a given B cell usually expresses either Igκ or Igλ, but not both (9). In mice, ∼95% of mature

J.H. Wang and C.T. Yan contributed equally to this paper.

The Rockefeller University Press $30.00
J. Exp. Med. Vol. 205 No. 13 3079-3090
www.jem.org/cgi/doi/10.1084/jem.20082271

B lymphocytes are Igκ$^+$, with the remainder being Igλ$^+$. In that context, *Igκ* assembly usually precedes that of *Igλ* (9). Thus, most Igκ$^+$ B cells contain *Igλ* in germline configuration, with *Igλ* rearrangements occurring in cells in which both *Igκ* alleles are rearranged out-of-frame or that harbor deletions of the Jκ segments, κ enhancer, and/or Cκ exons (9). Such deletions usually occur via rearrangement of Vκs or an RS heptamer in the Jκ-Cκ intron (IRS) to a bona fide RS 25 kb downstream of Cκ (3′RS) (10). Recent analyses suggest that *Igκ* deletions via 3′RS rearrangements may play a role in progression to *Igλ* rearrangement (11).

Expression of complete Ig (IgH/IgL) leads to IgM$^+$ B lymphocytes, which ultimately down-regulate RAG expression to enforce allelic exclusion (1). However, newly generated BM IgM$^+$ B lymphocytes that express autoreactive B cell receptors can maintain RAG expression and continue to rearrange *IgL* loci to generate new IgL chains in a tolerance process termed "receptor editing" (12–14). Receptor editing can replace rearranged *Igκ* loci with secondary productive *Igκ* rearrangements, as well as with nonfunctional *Igκ* rearrangements or *Igκ* deletions that may lead to *Igλ* rearrangement (12–14). Thus, Igλ$^+$ B cells can be generated developmentally from pre–B cells with two nonproductive *Igκ* rearrangements or via receptor editing from immature Igκ$^+$ B cells. Receptor editing is initiated in immature BM B cells (15, 16). Yet, several studies suggested *IgL* gene rearrangement, sometimes called "revision," in mouse and human peripheral B cells, including germinal center B cells (17–21). However, many peripheral mouse RAG$^+$ B lineage cells are pro– or pre–B cells that migrate to the periphery after immunization (22, 23), and knock-in reporter studies suggested that although RAG genes are expressed in B cells that have just migrated from the BM (24, 25), they are not reinduced in peripheral B cells once expression is terminated (25, 26).

After antigen stimulation, mature IgM$^+$ peripheral B cells can undergo IgH class switch recombination (CSR), a recombination/deletion process in which the IgH μ constant region exons (Cμ) are deleted and replaced by one of several sets of downstream C_H exons (e.g., Cγ, Cε, and Cα; referred to as C_H genes) (27), leading to switching from IgM to another Ig class (e.g., IgG, IgE, or IgA). The activation-induced cytidine deaminase (AID) initiates CSR (28) by deaminating cytidines in switch (S) regions (29), which are 1–10-kb repetitive sequences located 5′ of each C_H gene. AID-generated lesions within the donor Sμ and a downstream acceptor S region are processed into DSBs, which are end-joined to complete CSR (27). In contrast to V(D)J recombination, substantial CSR occurs in the absence of Xrcc4 or Lig4 (C-NHEJ) via an alternative end-joining (A-EJ) pathway strongly biased to use microhomology (30). However, CSR is significantly impaired in Xrcc4-deficient B cells owing to failure to join broken S regions because up to 20% of Xrcc4-deficient B cells activated for CSR in vitro have *IgH* chromosomal breaks, with a substantial portion participating in chromosomal translocations (30).

Inactivation of *Xrcc4* in mice results in impaired cellular proliferation and ionizing radiation sensitivity. Xrcc4 deficiency also results in extensive apoptosis of newly generated neurons and late embryonic death (6), both of which can be rescued by deficiency for the p53 tumor suppressor (31). In this context, p53 monitors the G1 cell cycle checkpoint, signaling apoptosis of certain cell types, such as neurons and progenitor lymphocytes, which harbor persistent DSBs (32). However, as p53 deficiency does not rescue defective NHEJ associated with Xrcc4 deficiency, Xrcc4/p53–double-deficient mice are still immunodeficient and inevitably succumb to pro–B cell lymphomas that harbor RAG-dependent complex translocations (33). These translocations usually join *IgH* on chromosome 12 to a region downstream of *c-myc* on chromosome 15, resulting in dicentric 12;15 translocations and *c-myc* amplification via breakage–fusion–bridge cycles (34). Such complex translocations are rare in human peripheral B cell lymphomas, which more frequently harbor reciprocal translocations that fuse *IgH*, or less frequently *IgL* loci, just upstream of *c-myc*, leading to ectopic *c-myc* activation (35).

In the current study, we have asked whether inactivation of C-NHEJ in WT or p53-deficient peripheral B cells leads to peripheral B cell lymphoma with CSR or V(D)J recombination-associated *IgH* or *IgL* locus translocations.

RESULTS

Inactivation of *Xrcc4* in p53-deficient peripheral B cells leads to novel B cell lymphomas

We previously inactivated *Xrcc4* specifically in transitional stage peripheral B cells by generating mice that harbored one copy of a loxP-flanked (floxed) *Xrcc4* allele (X^c) and one copy of an *Xrcc4*-null allele (X^-) plus a transgene that drives Cre recombinase expression via a *CD21* promoter (termed $CX^{c/-}$ mice) (30). CD21 proteins are expressed during B cell development at the time when immature transitional B cells differentiate into mature long-lived peripheral B cells, including marginal zone B cells, follicular B cells, B1a (CD5$^+$), and B1b cells (36). CD21cre mediates efficient Cre recombination in mature, but not immature, transitional B cells (37). Thus, $CX^{c/-}$ mice have normal IgM$^+$ splenic B cell numbers as *Xrcc4* is not deleted during early B cell developmental stages where V(D)J recombination occurs (30). Remarkably, $CX^{c/-}$ mice have a normal life span and are not cancer-prone (Fig. 1 A), despite high levels of general and *IgH*-specific genomic instability in ex vivo αCD40/IL-4–stimulated peripheral $CX^{c/-}$ B cells (30). Analogous to what we previously found for B lymphoid and neuronal progenitors (31), lack of $CX^{c/-}$ B cell transformation may reflect p53-dependent elimination of cells harboring DSBs and other types of genomic instability. To investigate this possibility, we bred $CX^{c/-}$ mice into a p53-deficient background to generate $CX^{c/-}P^{-/-}$ mice.

The majority of $CX^{c/-}P^{-/-}$ mice become moribund by 3.5–4.5 mo of age, with >50% succumbing to Xrcc4/p53-deficient B lineage lymphomas that present predominantly in the mesenteric lymph nodes and that had deleted *Xrcc4* (Fig. 1, A and B). The remaining $CX^{c/-}P^{-/-}$ mice succumbed to thymic lymphomas and sarcomas characteristic of p53 deficiency alone and which had not deleted *Xrcc4* (Fig. 1 B).

In contrast, none of the $CP^{-/-}$, $CX^{c/-}$, or $CX^{c/-}P^{+/-}$ littermates developed B lymphomas (Fig. 1, A and B). Of eight $CX^{c/-}P^{-/-}$ B lineage lymphomas (termed CXP lymphomas) characterized in detail, all were surface Ig negative (sIg^-) and all were $B220^+$, $CD43^{low}$, CD138/Syndecan-1^+, and $CD19^+$ (Fig. S1 A, available at http://www.jem.org/cgi/content/full/jem.20082271/DC1). In addition, all had clonal *IgH* and *Igκ* rearrangements and many had clonal *Igλ* rearrangements, even though they usually lacked expression of IgH and IgL proteins (Table S1; see below). RNA expression analyses indicated that *CXP* lymphomas lacked expression of λ5 and Vpre–B, two diagnostic early B cell markers, but did show very low-level RAG expression (Fig. S1, B and C, and not depicted). We also analyzed six additional Xrcc4/p53-deficient B lymphomas derived from $CX^{c/-}$ mice in which the p53 gene was also floxed ($CX^{c/-}P^{c/c}$) and found that the majority had a phenotype similar to $CX^{c/-}P^{-/-}$ lymphomas (Fig. S2 and Table S2). Likewise, eight additional $CX^{c/-}P^{-/-}$ B lymphomas that were also heterozygous for a mutation in the 3′ IgH regulatory region (CXPR lymphomas) had a similar phenotype, including lack of surface Ig expression (unpublished data). As expected, we found little or no evidence of *Xrcc4* deletion in sorted BM $B220^+IgM^-$ cells or in sorted $HSA^{high}CD21^{low}$ peripheral immature B cells, but essentially complete *Xrcc4* deletion in purified $HSA^{low}CD21^{high}$ mature splenic B cells (Fig. S3). By PCR, we occasionally observed very low levels of a product corresponding to *Xrcc4* deletion in BM and immature B cell samples, which theoretically may reflect very low-level deletion in earlier B cell stages, but which also may simply reflect recirculating peripheral B cells in the BM and/or low-level contamination of the sorted populations (unpublished data). Along with the appearance of these B lineage tumors being dependent on *Xrcc4* deletion via *CD21cre* expression at transitional B cell stage (Fig. 1 B and Fig. S3) (30), these phenotypic characterizations indicate that CXP lymphomas, despite lack of surface Ig expression, derive from peripheral B cells.

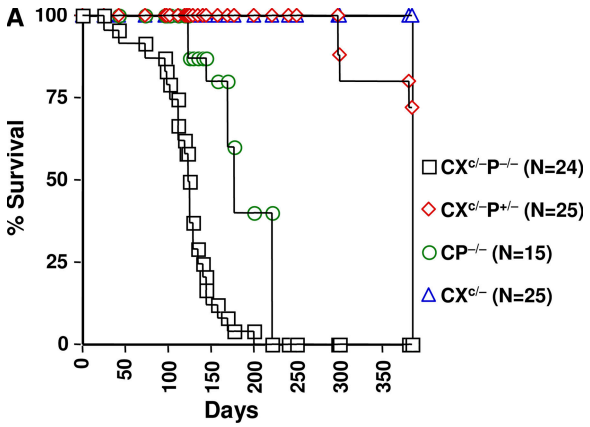

B **Characterization of Tumors**

No. of mice	Tumor	Xc floxed allele deleted
	Genotype ($CX^{c/-}P^{-/-}$)	
14	B cell lymphoma	Yes
1	B cell lymphoma	No
4*	Osteosarcoma	No
4*	Thymic lymphoma	No
5	nd	nd
	Genotype ($CP^{-/-}$)	
1	rhabdosarcoma	N/A
6	Thymic lymphoma	N/A

Figure 1. Establishment of the CXP B cell lymphoma model via conditional inactivation of *Xrcc4* in CD21Cre-expressing, p53-deficient mice. (A) Kaplan-Meier survival curve: percent survival of $CX^{c/-}P^{-/-}$ ($n = 24$); $CX^{c/-}P^{+/-}$ ($n = 25$); $CP^{-/-}$ ($n = 15$); and $CX^{c/-}$ ($n = 25$) mice versus age in days is shown. (B) Tumor types that developed in the indicated cohorts of $CX^{c/-}P^{-/-}$ and $CP^{-/-}$ mice. The number of mice that developed a given type of tumor is indicated at the left. Deletion of the floxed *Xrcc4* allele in given tumors is indicated at the right. nd, not determined; N/A, not applicable. The asterisk indicates $CX^{c/-}P^{-/-}$ mice that developed osteosarcoma or thymic lymphomas, in addition to B cell lymphomas.

IgH, *Igκ*, and *Igλ* rearrangements in CXP tumors

Recurrent sIg^- peripheral lymphomas have not been observed previously. To elucidate the basis for this striking phenotype, we first assayed for expression of IgH chains via Western blotting of tumor extracts. Most analyzed CXP B lymphomas lacked readily detectable IgH chain expression, although CXP62 expressed cytoplasmic γ chains (Fig. 2, B and C). Both normal and C-NHEJ–deficient pro–B lines display rearrangements of both J_H alleles (31). Assays of CXP tumor DNA for J_H rearrangements via Southern blotting revealed that all primary CXP tumors showed J_H rearrangements, along with varying degrees of a germline J_H band (Fig. 2 A). However, the germline band usually occurred in low levels and was often further reduced in passaged tumors (unpublished data), indicating derivation from non–B lineage cells within the tumor. Despite lack of detectable IgH expression, molecular cloning demonstrated that CXP tumors contained structurally normal in-frame or out-of-frame V(D)J rearrangements, indicating that they occurred before *Xrcc4* inactivation (see the following section). Finally, most CXP tumors had rearrangements in or around *IgH* S regions. At least five out of eight CXP tumors had clonal Sμ/Cμ rearrangements; three had one or more clonal Sα rearrangements of which one was molecularly cloned (from CXP68) and found to be an Sγ2a to Sα rearrangement; one CXP tumor had an Sγ2b rearrangement; and another had a clonal Sγ3 rearrangement in addition to the Sγ2a to Sα rearrangement (Table S1 and Fig. S4, A and B, available at http://www.jem.org/cgi/content/full/jem.20082271/DC1). Thus, most CXP tumors derived from peripheral B cells that had attempted *IgH* CSR.

No analyzed CXP tumor expressed readily detectable Igκ and Igλ chains (Fig. 2 B and not depicted). Approximately 60% of normal B cells have one productively rearranged *Igκ* allele and one germline allele, and ∼40% have one productive and one nonproductively rearranged or deleted Jκ allele (38).

We assayed for Jκ rearrangements by Southern blotting and found that all eight analyzed CXP tumors lacked both copies of the Jκ locus (Fig. 3 A and Fig. S5 A, available at http://www.jem.org/cgi/content/full/jem.20082271/DC1). Although there was a variable level of a germline-sized Jκ band, the level was far below that expected for a single germline allele and roughly correlated with that of contaminating nonlymphoid DNA as judged by the J_H Southern blot (Fig. 2 A). Southern blotting revealed that CXP tumors also lacked both copies of the Cκ exons (Fig. 3 A). We tested for downstream RS rearrangement in CXP tumors via Southern blotting and found rearrangement and/or deletion of the 3′RS sequences in all analyzed tumors (Fig. 3 A and Fig. S5 A). As normal 3′RS rearrangements do not result in deletions larger than a few nucleotides (39), we tested the hypothesis that 3′RS rearrangements in CXP lymphomas had occurred after *Xrcc4* inactivation by cloning and sequencing rearrangements. Of three RS rearrangements isolated, two had apparent Vκ and 3′RS region junctions accompanied by large deletions (30–80 bp into Vκ and 26–43 bp beyond 3′RS sequence), whereas the other had a normal Vκ to 3′RS join (Fig. S5 B). In addition, Southern blotting with a 3′RS probe showed CXP163 had an aberrant RS rearrangement with a large deletion (>4 kb) downstream of the 3′RS sequence (Fig. S5 C). Southern blotting also showed that a significant proportion of $CX^{c/-}P^{c/c}$ B lymphomas (four out of six; Fig. S2) and CXPR B lymphomas (five out of eight; not depicted) had deleted one or both *Igκ* alleles. We conclude that deletional *Igκ* 3′RS rearrangements in CXP tumors are reminiscent of those associated with attempted V(D)J joining in the absence of C-NHEJ, suggesting they occurred in progenitors of CXP tumors subsequent to *Xrcc4* inactivation via *CD21cre* expression.

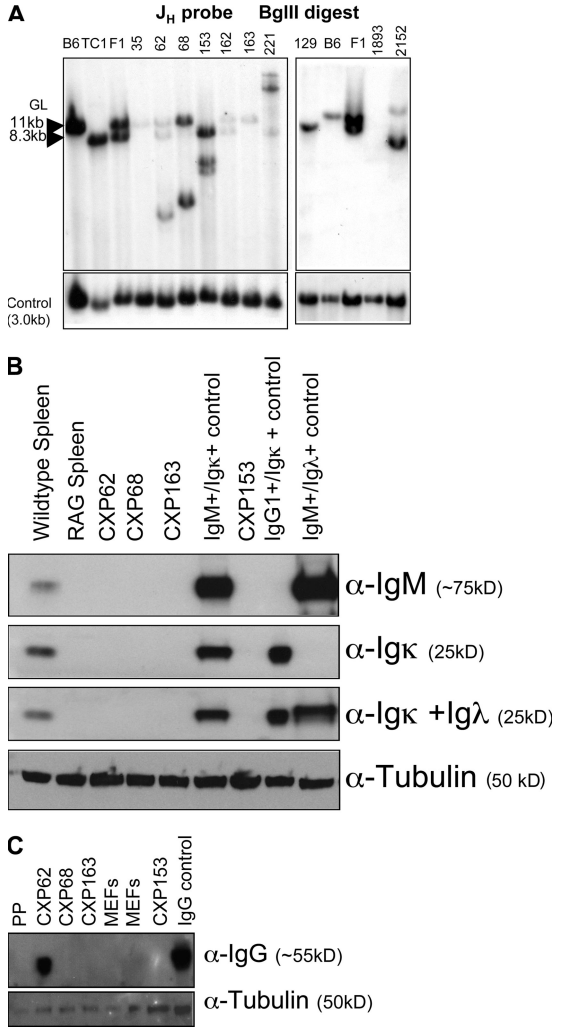

Figure 2. CXP lymphomas harbor clonal J_H rearrangements, but do not express IgM or IgL chains. (A) Southern blot analyses of CXP lymphoma genomic DNA samples for rearrangement or deletion of J_H loci (representative of at least two separate analyses for each sample). (B) Western blot analyses of CXP lymphoma cellular extracts for expression of μ heavy chain and κ or λ light chains using HRP-conjugated anti-IgM (μ heavy chain specific), anti-κ, or anti-λ antibodies, respectively. (C) Western blot analyses of CXP lymphoma cellular extracts for expression of γ heavy chains using HRP-conjugated anti–mouse IgG antibody. An α-tubulin antibody was used to generate a loading control in both panels. PP indicates extracts from Peyer's patches. Data presented in this figure shows results representative of two or three independent sets of analyses.

Complete *Igκ* deletion is generally observed in a subset of mouse peripheral $Ig\lambda^+$ B cells (39). Therefore, we assayed CXP lymphoma DNA by Southern blotting with probes to detect VλJλ rearrangements within both Igλ clusters (Fig. S5 D). These analyses demonstrated that at least six out of nine assayed CXP or $CX^{c/-}P^{c/c}$ B cell lymphomas had clear-cut *Igλ* rearrangements, with CXP62, 162, and 163 showing rearrangements of both alleles (Fig. S5, A and D). Southern blotting analyses also showed that several analyzed CXPR B lymphomas had *Igλ* rearrangements (unpublished data). To elucidate the nature of the *Igλ* rearrangements in CXP tumors, we performed PCR using Vλ1/Vλ2- and Jλ1/Jλ2-specific primers to isolate six different rearrangements involving one or the other Jλ cluster (Fig. 3 B and Fig. S5 E). Nearly all isolated *Igλ* rearrangements involved joining of sequences in or upstream of a Vλ to sequences in or downstream of a Jλ, with the majority of breakpoints leading to deletions larger than the few basepair deletions observed from one or both segments in normal VλJλ joins (Fig. 3 B and Fig. S5 E) (40). As PCR only allows isolation of junctions within the primer boundaries, we cloned several *Igλ* rearrangements from genomic phage libraries generated from CXP163 and CXP162 DNA and identified a deletional rearrangement that went ∼2.8-kb and ∼800-bp, respectively, beyond the Vλ1 and Jλ1 segments, as well as aberrantly deleted RS rearrangements (Fig. 3 B and Fig. S5 E). Overall, the observed pattern of *Igλ* rearrangements in CXP lymphomas, namely large deletions from the participating segments on one or both sides of the join, is fully consistent with the types of junctions previously characterized for attempted V(D)J recombination of endogenous loci in C-NHEJ–deficient progenitor B or T lymphocytes (3, 41). Therefore, CXP tumors appear to arise from B cells that attempted *Igλ* rearrangement subsequent to *Xrcc4* deletion via *CD21cre* expression.

C-NHEJ suppresses oncogenic CSR-related translocations between *IgH* and *c-myc*

Spectral karyotyping (SKY) revealed that six out of eight characterized CXP tumors (CXP68, 153, 162, 163, 221, and 2152) harbored clonal translocations between chromosomes 12 and 15, possibly involving *IgH* (Chr12) and *c-myc* (Chr15) loci (Fig. 4 A, Table S3, and Fig. S6 A, available at http://www.jem.org/cgi/content/full/jem.20082271/DC1). To test this possibility, we performed fluorescence in situ hybridization (FISH) with 5′ and 3′ *IgH* BAC probes plus a BAC probe containing *c-myc* (Fig. 4 A). These analyses demonstrated that 5 out of 6 tumors (CXP68, 153, 162, 163, and 2152) harbored reciprocal t(12;15) and t(15;12) translocations in which the centromeric portion (C_H) of *IgH* (3′ IgH probe) was fused proximal to the telomeric portion of Chr15 in or around *c-myc* (c-myc BAC probe) to yield the t(12;15) translocation, and the telomeric (V_H) portion of *IgH* (5′ IgH probe) was fused proximal to the centromeric portion of Chr15 in or just upstream of *c-myc* to yield the reciprocal t(15;12) translocation (Fig. 4 A and Fig. S6 A). CXP221 harbored a clonal t(12;15) translocation involving *IgH* and *c-myc* loc, but lacked the reciprocal t(15;12) translocation, and instead contained a clonal t(15;7) translocation (Fig. S6 A). Based on FISH, neither *c-myc* nor *IgH* appeared amplified in CXP tumors. Similar to CXP tumors, three out of four analyzed $CX^{c/-}P^{c/c}$ B lymphomas and six out of six CXPR tumors analyzed had translocations involving chromosomes 12 and 15 that involved the *IgH* and *c-myc* loci (Fig. S6 A, Table S4, and not depicted).

To further analyze CXP B lymphoma t(12;15) and t(15;12) translocation junctions, we performed Southern blotting with probes within or just upstream of *c-myc* (Fig. S6 B). These analyses demonstrated that the six CXP lymphomas with t(12;15) translocations had clonal rearrangements in or

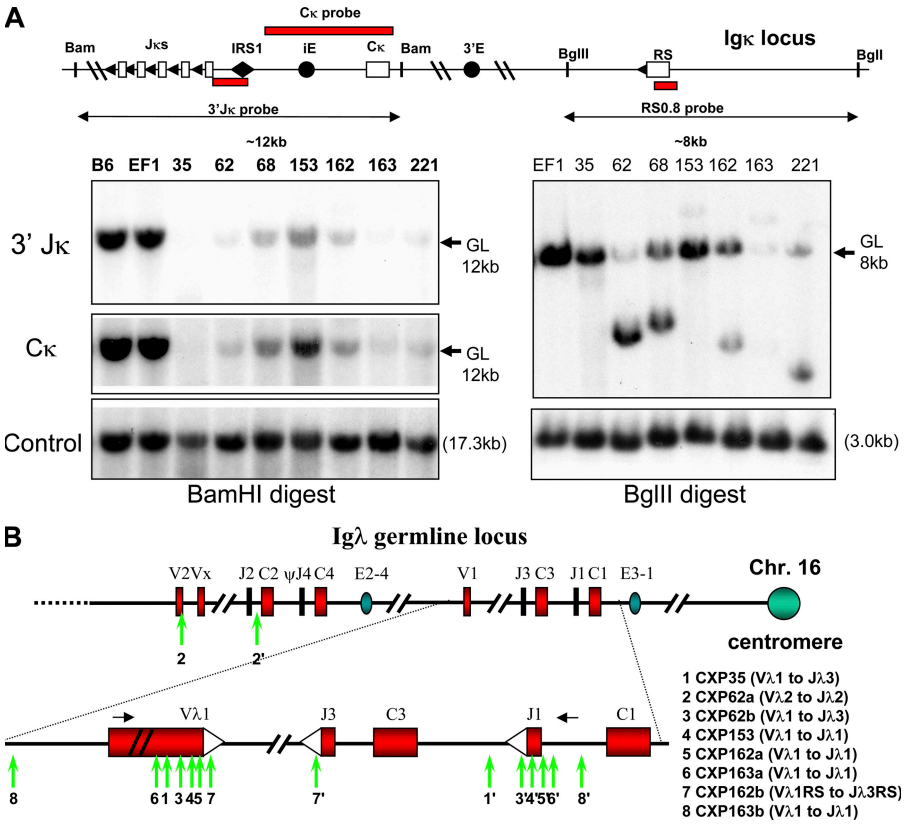

Figure 3. Aberrant IgL rearrangements in CXP lymphomas. (A, right) Southern blot analyses for Jκ rearrangements in CXP lymphoma genomic DNA using BamHI digestion and the 3′ Jκ and Cκ probes indicated in schematic at top of panel. (left) Southern blot analysis for RS rearrangements in CXP lymphoma DNA using BglII digestion and the indicated RS0.8 probe. Germline (GL) bands and their known sizes are indicated (arrows). Blots were performed at least two times. (B) Assays for rearrangements occurring in or near Vλ and Jλ segments in DNA samples from CXP lymphomas. Rearrangements were isolated either by PCR or by cloning from λ-phage genomic DNA libraries generated from individual tumor DNA samples. Black arrows denote the position of the PCR primers used for the studies, and primer sequences are indicated in the Materials and methods section. The two breakpoints for a given rearrangement in the vicinity of Vλ and Jλ in a particular tumor are indicated by the same number with the breakpoint in the Jλ region indicated by a (′) symbol. PCR analyses were performed at least three times from one or multiple independent DNA samples from a given tumor. PCR fragments were subcloned into the pGEM vector, and 10–20 subclones were sequenced. Identical rearrangements that were isolated from >80% of the subclones were scored as clonal rearrangements. At least two independent phage clones were isolated from each genomic library and the junctions found in phage clones were independently confirmed as clonal junctions in a given tumor by PCR analyses of tumor cell DNA. Sequences of cloned Vλ and Jλ rearrangement junctions are shown in Fig. S5E.

around *c-myc* (Fig. S6 B and not depicted), with one additional tumor that lacks a t(12;15) translocation (CXP62; detailed in the following section), also showing a clonal *c-myc* rearrangement (Fig. S6 B). Southern blotting confirmed that none of the CXP tumors had amplified *c-myc* (Fig. S6 B). Northern blotting with a *c-myc* probe further demonstrated that all CXP tumors with t(12;15) translocations had greatly increased *c-myc* expression, indicating ectopic overexpression from a single copy of the translocated *c-myc* gene (Fig. S6 C). Of note, only two CXP tumors lacked t(12;15) translocations; however, one (CXP62) activated *c-myc* via an *Igλ/c-myc* translocation (see below) and the other (CXP35) had a complex Chr12 translocation that resulted in *N-myc* amplification and overexpression (Fig. S6 C and Fig. S7 A, available at http://www.jem.org/cgi/content/full/jem.20082271/DC1) reminiscent of that observed in Artemis/p53-deficient pro–B cell tumors (42). Thus, all CXP tumors overexpressed a *myc* family gene.

To further elucidate *IgH/c-myc* translocations in CXP tumors, we isolated translocation junctions by screening genomic DNA libraries from individual tumors. Nucleotide sequence analyses showed that all five characterized junctions corresponded to translocations between *IgH* and *c-myc* (Fig. 4 B and Fig. S6 D). All junctions on Chr12 (Fig. 4 B, red), including those associated with both t(12;15) and t(15;12) occurred within *IgH*, most in the C_H region within or around S regions consistent with derivation via aberrant CSR. The CXP153 t(12;15) junction linked Sγ1 to sequences just 5′ of *c-myc* (junction 1, CXP153), whereas the t(15;12) linked Sμ to sequences in the first intron of *c-myc* (Fig. 4 B and Fig. S6 D). The CXP163 t(12;15) junction linked Iμ to a sequence

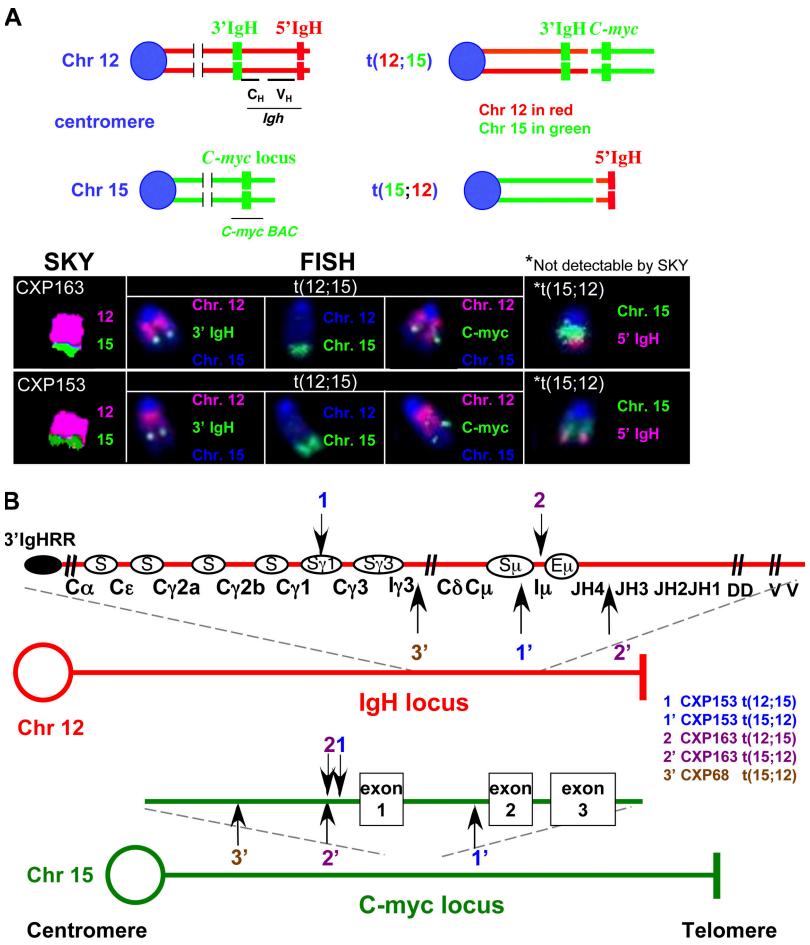

Figure 4. Reciprocal *IgH/c-myc* translocations in CXP lymphoma. (A) SKY, FISH, and chromosome paint analyses (Chr12 pink, Chr15 green) for *IgH/c-myc* translocations in CXP163 and CXP153. A *3′ IgH* BAC (light green) and a *c-myc* BAC (light green) were used in combination with chromosome paints to detect t(12;15) translocations. The t(15;12) translocation, not detectable by SKY, was visualized using the 5′ *IgH* BAC (pink) and a Chr15 paint (green). At least 15 metaphase spreads were analyzed for SKY, FISH, and chromosomal paints, respectively, for each CXP tumor. Translocations shown were observed in the majority of metaphases, and were scored as clonal if observed in >80% of metaphases. (B) Schematic of *IgH/c-myc* translocation breakpoint junctions cloned and sequenced from λ-phage tumor genomic DNA libraries. At least two independent phage clones were isolated from each genomic DNA library, and breakpoint junctions identified within them were further independently confirmed by PCR and sequencing from the appropriate tumor DNA samples. The numbers on the top indicate t(12;15) translocation breakpoints and the same numbers containing a (′) on the bottom indicate the "reciprocal" t(15;12) translocation breakpoints in the corresponding tumor: CXP153 (junction 1 and 1′), 163 (junction 2 and 2′), and 68 (junction 3′).

288 bp upstream of *c-myc* exon 1, and the t(15;12) linked sequences between J_{H3} and J_{H4} to sequences 289 bp upstream of *c-myc* exon 1 (Fig. 4 B and Fig. S6 D); notably, the CXP163 t(15;12) junction occurred downstream of a nonproductive $V_H(D)J_H$ rearrangement (Fig. 5 B), indicating that it did not happen during V(D)J recombination and, rather, may have resulted in association with a large deletion from a breakpoint downstream in Iμ-Sμ region. Finally, the t(15;12) CXP68 junction linked sequences near Iγ3 to sequences 1.4-kb upstream of *c-myc* exon 1 (Fig. 4 B), again, likely resulting from attempted CSR to Sγ3. Four of these five cloned junctions contained junctional microhomology suggestive of A-EJ (Fig. S6 D). Overall, CXP *IgH/c-myc* translocations are remarkably similar to those of human sporadic Burkitt's lymphoma that fuse *IgH* S regions upstream of *c-myc*.

Because of the location of the characterized translocation junctions downstream of the *IgH* J_H region, we considered the possibility that many CXP tumors were sIg^- because they separated a productive $V_H(D)J_H$ exon from the C_H region. In this context, two out of three analyzed CXP tumors with *IgH/c-myc* translocations (CXP68 and CXP153) contained an in-frame (productive) $V_H(D)J_H$ rearrangement fused to the *c-myc* locus on Chr15; whereas the other (CXP163) involved a translocated nonproductive $V_H(D)J_H$ rearrangement (Fig. 5, A–C). In CXP163, which has the nonproductive $V_H(D)J_H$ translocated to *c-myc*, the other Chr12 was involved in a t(12;16) translocation that may have resulted in loss of the presumably productive $V_H(D)J_H$ exon, as the breakpoint is centromeric to *IgH* (Fig. 7 A and Fig. S7 A). Of the four $V_H(D)J_H$ junctions and downstream flanks sequenced (3,884 bp), one carried two somatic point mutations and the other three lacked mutations (unpublished data). Finally, cloned $V_H(D)J_H$ rearrangements appeared normal in respect to junctional deletions (Fig. 5, A–D), indicating they occurred in C-NHEJ–proficient cells. Therefore, primary V(D)J recombination at the *IgH* locus was normal in B lineage cells that gave rise to CXP lymphomas.

CXP lymphomas frequently harbor *Igλ* translocations

SKY analyses demonstrated that five out of eight characterized CXP B lymphomas (CXP35, 62, 68, 162, and 163), many of the same ones that harbored translocations between chromosomes 12 and 15, harbored Chr16 translocations to various other chromosomes with two others (CXP153 and 2152) harboring nonclonal Chr16 translocations (Fig. 6 A, Table S3, and Fig. S7 A). In contrast to the Chr12 translocations, all but one Chr16 translocation (i.e., CXP62) appeared nonreciprocal (Fig. 6 A and Fig. S7 A), similar to RAG-initiated oncogenic *IgH* translocations in Xrcc4/p53–deficient pro–B lymphomas (34). As the *Igλ* locus is on Chr16, we used FISH with three different BAC probes covering the *Igλ* locus to determine whether the Chr16 breakpoints involved *Igλ* (Fig. 6 A; P12 is centromeric to *Igλ*, E14 spans both *Igλ* clusters, P9 is telomeric to *Igλ*). These analyses revealed that all five Chr16 breakpoints occurred directly within various regions of *Igλ* (Fig. 6 A and Fig. S7 A). We also observed clonal translocations of Chr6 (which contains *Igκ*) in one of eight CXP tumors and in two of four characterized $CX^{c/-}P^{c/c}$ B lymphomas (Tables S3 and S4). Notably two tumors (CXP162 and $CX^{c/-}P^{c/c}$ 1893) harbored clonal t(6;16) translocations that fused *Igλ* to Chr6. However, cytogenetic analyses indicated that these t(6;16) translocations did not harbor *Igκ* (Fig. S7 A), although *Igκ* may still have been involved and deleted during joining (see the following section).

Characterization of several *Igλ* breakpoints by FISH and/or molecular cloning revealed partner loci and showed that sequences around translocation junctions lacked somatic hypermutation (SHM; Fig. S7 B and not depicted). By SKY, the CXP62 tumor, which was the only one that did not activate a *myc*-family gene by an *IgH* translocation, contained reciprocal t(16;15) and t(15;16) translocations, which juxtaposed the *Igλ* P12 BAC probe to the telomeric portion of Chr15 in

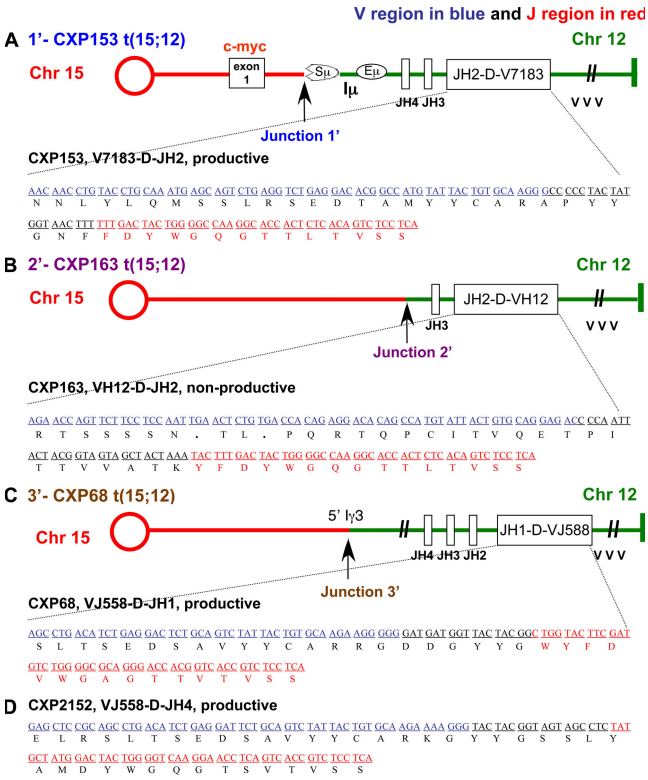

Figure 5. CXP lymphomas harbor normal V(D)J rearrangements in IgH locus. Nucleotide sequence analysis of primary $V_H(D)J_H$ rearrangements cloned from the following: CXP153 by both λ-phage library and PCR (A); CXP163 by λ-phage library (B); CXP68 by PCR (C); and CXP2152 by PCR (D). Additional sequence analyses revealed that CXP153 had a productive V7183-D-JH2 rearrangement juxtaposed into to the first intron of *c-myc* and CXP163 has a nonproductive VH12-D-JH2 rearrangement juxtaposed to the sequence upstream of *c-myc* exon1. V regions are shown in blue and J regions in red. The open reading frame is indicated under the DNA sequence. PCR analyses were performed at least three times from one or multiple independent tumor DNA samples. PCR fragments were subcloned into pGEM vector, 10–20 subclones were sequenced, and identical rearrangements observed in >80% clones were scored as clonal rearrangements.

the t(16;15) translocation, and the *Igλ* P9 and E14 BAC probes to the centromeric portion of Chr15 in the t(15;16) translocation (Fig. 6 A). Based on analyses of cloned junctions, the t(16;15) translocation fused sequences upstream of Jλ1 to sequences 5′ of *c-myc* exon 1 (Fig. 6 B and Fig. S7 B), which led to high level expression of *c-myc* transcripts (Fig. S6 C), whereas the t(15;16) translocation contained the reciprocal product (Fig. S7 B). FISH analyses of the complex t(12;12;16) translocation that led to *N-myc* amplification in CXP35 revealed that it involved both *Igλ* and *IgH* loci (Fig. S7 A). Likewise, FISH analyses of the nonreciprocal t(12;16) CXP68 translocation revealed colocalization of 3′ *IgH* and *Igλ* P9 BAC probes at the junction (Fig. 6 A). By phage cloning, we mapped the CXP68 breakpoint to Cδ in *IgH* and just 3′ of Jλ2 in *Igλ* (Fig. 6 B and Fig. S7 B).

Comparative genomic hybridization analyses of CXP tumors

We used comparative genomic hybridization (CGH) to assay for sequence copy number differences among tumor and control tissues samples. Among the four samples derived from the CXP or $CX^{c/-}P^{c/c}$ cohort, three had clearly lost one copy of either the entire Chr6 or a large region of Chr6, with the boundary of the loss occurring near or spanning *Igκ* (Fig. S8, available at http://www.jem.org/cgi/content/full/jem.20082271/DC1, and not depicted). Out of nine CXPR B lymphoma DNAs analyzed, seven again had a clear loss of one copy of the entire Chr6 or a large region that in two extended directly from *Igκ* (Fig. S8 and not depicted). CGH also showed focal deletion of *Igκ* in most analyzed CXP, $CX^{c/-}P^{c/c}$, or CXPR tumors (Fig. S8 and not depicted), which is consistent with results of Southern blotting

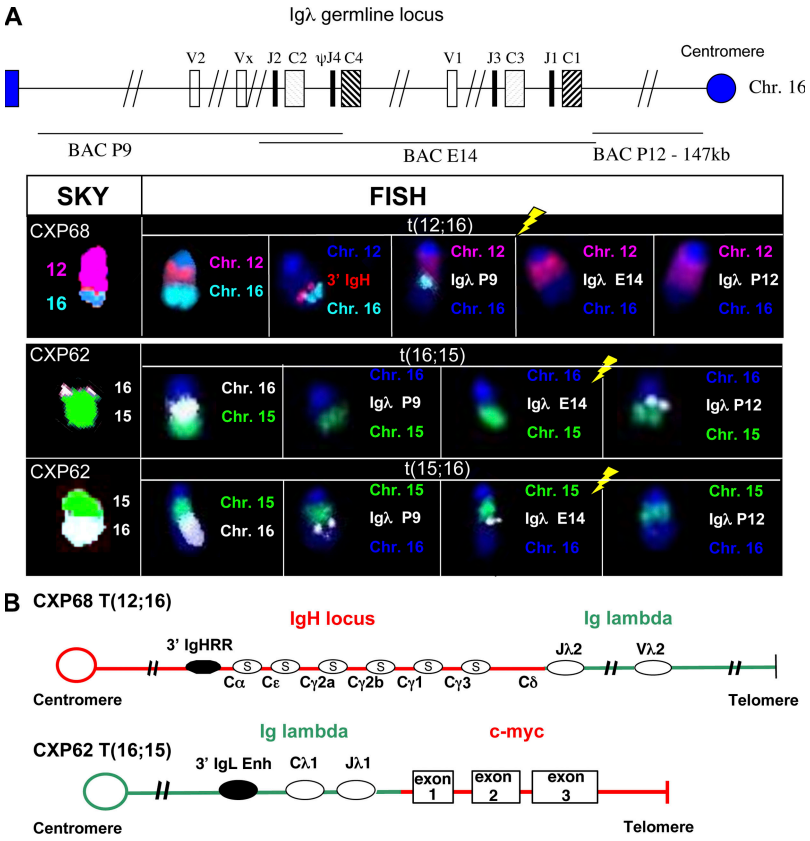

Figure 6. Recurrent chromosome 16 translocations. (A) SKY/FISH analyses of *Igλ* translocations in CXP lymphomas. (A, top) schematic map of *Igλ* locus in germline configuration and the location of the three BACs used for FISH (P9, E14, and P12).(bottom) SKY revealed a t(12;16) translocation in CXP68, and a reciprocal t(16;15) and t(15;16) translocation in CXP62. FISH and chromosome paints (Chr12 pink, Chr16 light blue or white, Chr15 green) showed the breakpoints of Chr16 translocations occurred in different regions of the *Igλ* locus, indicated by yellow lightning symbols over metaphases hybridized with different *Igλ* BACs. *3′ IgH* (pink) and *P9* (light blue) BACs were colocalized at the junction of t(12;16) in CXP68. CXP62 has a reciprocal translocation with P12 BAC (white) on the der(16)t(16;15) and E14 and P9 (white) BACs on the der(15)t(15;16). At least 15 metaphase spreads were analyzed for each of the cytogenetic analyses, and representative clonal translocations observed in >80% of the metaphases are shown. (B, top) Cloning of t(12;16) breakpoints from a genomic library made from CXP68 DNA. Nucleotide sequence analyses of cloned junction (shown in Fig. S7 B) indicated breakpoints occurred between Cδ in IgH and Jλ2 in Igλ locus. (bottom) Cloning of t(16; 15) breakpoints from a genomic library made from CXP62 DNA. Nucleotide sequence analyses indicated breakpoints occurred between sequences upstream of *c-myc* exon 1 and Jλ1 with 3′ *Igλ* enhancer in close proximity. At least two independent phage clones were isolated from each genomic library and the junctions found in phage clones were independently confirmed as clonal junctions in a given tumor by PCR analyses of tumor DNA sample. Fig. S7 is available at http://www.jem.org/cgi/content/full/jem.20082271/DC1.

analyses. In contrast, three thymic lymphomas and two forebrain tumors, most likely of glial origin, analyzed did not show loss of Chr6 or a large region proximal to *Igκ* (Fig. S8 and not depicted).

DISCUSSION

Xrcc4 deficiency in peripheral B cells does not predispose to B cell lymphoma, despite dramatic *IgH* instability in Xrcc4-deficient B cells activated for CSR by treatment with αCD40 plus IL-4 (30). In this context, αCD40 plus IL-4–activated splenic CXP B cells had at most a very modest increase in *IgH* breaks compared with activated Xrcc4-deficient peripheral B cells (28 ± 13% versus 17 ± 7% of metaphases containing *IgH* breaks). Yet, *CD21cre* deletion of *Xrcc4* in p53-deficient peripheral B cells, or deletion of both genes in peripheral B cells, recurrently led to sIg^- B lymphomas that harbor activated *myc*, likely reflecting the critical role of p53 in eliminating B cells with activated *c-myc* expression and/or eliminating B cells with high genomic instability (33, 43, 44). CXP B lymphomas are remarkable in several ways. First, most CXP lymphomas arise from B cells that have attempted *IgH* CSR and a majority appear to arise from B cells that have undergone receptor editing, with both processes occurring after *Xrcc4* inactivation by CD21Cre. Second, many CXP tumors harbored two separate, clonal translocations that, respectively, involved *IgH* and *IgL* loci. Occurrence of clonal *IgH* and *IgL* translocations in the same tumor may reflect dual CSR and editing activities of B cells from which they arose. In this context, some CXP lymphomas had clonal translocations that fused *IgH* and *Igλ*, clearly indicating simultaneous presence of breaks in both loci in tumor progenitors. As outlined below, these unusual features of CXP tumors have novel implications for B cell developmental processes and for oncogenic translocation mechanisms.

Germline Xrcc4 plus p53 deficiency in mice leads to pro–B lymphomas with RAG-dependent translocations that fuse J_H sequences to sequences far downstream of c-*myc,* resulting in dicentric chromosomes and *c-myc* activation via breakage-fusion-bridge amplification (34). Thus, it is remarkable that inactivation of same two genes in mature B cells recurrently leads to ectopic activation of a single copy *c-myc* gene by fusion of *IgH* into its upstream region, analogous to similar *IgH/c-myc* translocations in human Burkitt's lymphoma and diffuse large B cell lymphomas (35). In pristane- or IL-6–induced mouse plasmacytomas, similar *IgH/c-myc* translocations occur and are initiated by AID (45, 46). In this context, CXP lymphoma *IgH/c-myc* translocations occur in and around *IgH* S regions and downstream of normal $V_H(D)J_H$ exons, indicating their likely selection from the abundant pool of *IgH* translocations that result from aberrant CSR in activated Xrcc4-deficient peripheral B cells (30). As the intronic IgH enhancer is generally absent from CXP *IgH/c-myc* translocations, long-range 3′ IgH regulatory region activity (47), or that of unknown *IgH* regulatory elements, may ectopically activate *c-myc*. The recurrent differences in *IgH/c-myc* translocations in Xrcc4/p53-deficient pro–B versus CXP peripheral B cell tumors might reflect RAG versus AID-dependent DSB initiation in *IgH* and/or *c-myc*, other differential stage-specific mechanisms that lead to DSBs in and around *c-myc*, stage-specific differences in nuclear localization of *IgH* and *c-myc* loci, or mechanisms that differentially activate *c-myc* after translocation, including stage-specific IgH enhancer activities. As both Xrcc4/p53-deficient pro–B and CXP peripheral B cell lymphomas frequently have *IgH/c-myc* junctions that appear to be mediated by A-EJ, repair pathway choice is not likely to be a major factor in generating a particular form of translocation. Given the uniform and recurrent *IgH/c-myc* translocations, the CXP B lymphoma system should allow putative roles of cis elements and other factors to be tested.

CXP lymphomas also frequently harbor chromosome 16 translocations that involve aberrant V(D)J recombination of *Igλ* after *Xrcc4* deletion. At least one CXP *Igλ* translocation was oncogenic. CXP62 had reciprocal t(15;16) and t(16;15) translocations, the latter of which fused the downstream portion of *Igλ* to sequences just upstream of *c-myc*, resulting in ectopic *c-myc* activation, reminiscent of *Igλ/c-myc* translocations observed in certain human B lymphomas (35). Characterization of additional CXP *Igλ* translocations may lead to identification of additional oncogenes. Notably, we also observe loss of all or part of one copy of chromosome 6 with some large deletions extending from the vicinity of *Igκ*. The latter findings suggest that rearrangements of *Igκ*, likely in association with aberrant editing, may also lead to translocations or chromosome loss. In the latter context, unrepaired DSBs can lead to chromosome loss in yeast (48). The frequent loss of all or a large portion of chromosome 6 in CXP tumors is striking and suggests a potential role in etiology of these tumors, perhaps by deletion of a tumor suppressor sequence.

More than 95% of mouse peripheral B cells express Igκ and, correspondingly, have VκJκ joins on one or both *Igκ* alleles and *Igλ* in germline configuration (9). A small percentage of mouse B cells express Igλ, and these have *Igκ* alleles that are nonproductively rearranged or deleted by 3′RS or related rearrangements (39, 49). Notably, Igλ-expressing mouse B cells frequently arise via receptor editing, often in the context of *Igκ* deletion via 3′RS rearrangement (39). Thus, it is striking that CXP lymphomas frequently had clonal *Igκ* deletions via aberrant Vκ to 3′RS rearrangements and aberrant Vλ to Jλ rearrangements, with both types of rearrangements occurring subsequent to *CD21cre* expression. Based on these findings, we speculate that a common CXP tumor progenitor derives from an Igκ-expressing B cell that attempted receptor editing subsequent to *Xrcc4* deletion. Attempted editing in the absence of Xrcc4 would lead to aberrant rearrangement/deletion of *Igκ* and progression to *Igλ* rearrangement, which also would be aberrant. Thus, editing Xrcc4-deficient B cells would lose IgL expression caused by inability to undergo productive IgL editing.

As a working model, we suggest that aberrant receptor editing in CXP tumor progenitors generates an initial transforming event and/or activates aberrant CSR through loss of parts of chromosome 6 or translocations of *Igλ*. Aberrant

CSR in the absence of Xrcc4 would lead to a high level of *IgH* translocations (30), including *IgH/c-myc* translocations that would complete the transformation process. In the case of the CXP tumor that harbors an *Igλ/c-myc* instead of an *IgH/c-myc* translocation, the former may have been sufficient to fully transform the cells. This scenario provides a potential role for chromosome 6 losses, and also could explain why all CXP *Igλ* translocations are not clearly oncogenic, why some CXP *Igλ* translocations have *IgH* as a partner, and why CXP *IgH* translocations can involve either productive or nonproductive *IgH* alleles.

Receptor editing is generally thought to occur in immature B cells in the BM (16); yet a substantial fraction of CXP tumor progenitors appear to have both breaks associated with attempted editing of the *Igλ* locus and breaks associated with attempted *IgH* CSR. In this regard, BM immature B cells in quasimonoclonal (QM) mice can express both AID and RAG1/2 (50), although other studies of developing B cells in WT mice concluded that AID is not expressed in BM B cells (51). QM mice harbor a productive IgH knock-in V(D)J allele and a homozygous gene-targeted deletion of both Jκ alleles and, thus, only have Igλ-producing B cells (52). The striking similarities between immature QM B cells and proposed CXP tumor progenitors suggest a potential relationship. In this regard, CXP tumor progenitors might derive from an undetected, low-level population of CD21cre-expressing BM immature B cells that delete *Xrcc4* and undergo aberrant editing and CSR before migration to the periphery. However, we note that CXP tumors arise in the periphery, have features of peripheral B cells, and harbor clonal *Igκ* and *Igλ* rearrangements, as well as *IgH* CSR-associated rearrangements that occurred subsequent to CD21cre expression. Conceivably, the *Igλ* breaks that lead to translocations found in CXP tumor progenitors might reflect RAG-initiated breaks in BM developing B cells that persist because of p53 deficiency, as observed for RAG-initiated *IgH* breaks in ATM-deficient or 53BP1/p53–double-deficient pro–B cells (53, 54). However, we also observed dual *IgH* and Igλ translocations in a $CX^{c/-}P^{c/c}$ tumor in which both *p53* and *Xrcc4* were deleted peripherally. Therefore, we must consider the alternative possibility that CXP tumors arise from peripheral B cells driven into editing. Such cells might also participate in extrafollicular responses in which CSR occurs with limited SHM (55), a possibility consistent with most CXP tumor IgH variable region exons lacking SHM.

Transitional B cell populations express very low levels of RAG upon arrival in the periphery, with RAG expression being essentially undetectable in more mature splenic B cell populations (24, 25). Thus, if the RAG breaks in CXP tumor progenitors, indeed, are generated in the periphery, it remains to be determined in what cell type they occur and how apparently low-level RAG expression could generate them. Given that CXP progenitors nearly all arise from cells that harbor *IgH/c-myc* translocations, it is quite striking that CXP tumors do not arise from sIg^+ B cells simply in the context of aberrant CSR. Indeed, the recurrent occurrence of sIg^- lymphomas with aberrant *Igκ* and *Igλ* rearrangements and translocations indicates that inability to productively complete receptor editing confers a major predisposition to transformation of peripheral CXP B cells. Perhaps editing CXP B cells represent a larger fraction of the CD21-expressing B cell pool than anticipated or are enriched in certain locations. For example, receptor editing might especially contribute to antibody diversification in B cells of the gut-associated lymphoid tissue (e.g., mesenteric lymph nodes), where the CXP tumors appear to arise most frequently and in which lymphocytes are chronically activated and driven into immune responses by products of the gut microflora.

MATERIALS AND METHODS

Mice. *CD21cre/Xrcc4*$^{c/-}$ mice were generated as previously described (30) and crossed into p53 germline-deficient mice (56) or mice carrying conditional p53 alleles (57). Animal work was approved by the Institutional Animal Care and Use Committee of Children's Hospital Boston.

Southern, Northern, and Western blot. Genomic DNA was isolated from tumor masses or normal tissues from control mice, and Southern blotting was performed as previously described (58). 3′Jκ probe was a 1-kb XbaI–HindIII fragment from plasmid pSPIg8 containing the Jκ and Cκ region (59), or generated by PCR using the following primers: 3′ Jκ5, 5′-CATCCAAGAGATTGGATCGGAGAATAAGCA-3′; MA35, 5′-AACACTGGATAAAGCAGTTTATGCCCTTTC-3′; and plasmid pSPIg8 as template. Cκ probe was a 1.7-kb HindIII–BglII fragment covering the Cκ region. RS probes were previously described (60). RNA samples were extracted from tumor masses or normal tissues from control mice using TriPure Isolation Reagent (Roche). Northern blotting was performed following a standard protocol. Western blotting was performed using HRP-conjugated antibodies at 1:1,000 dilution (HRP goat anti–mouse IgM [μ chain–specific antibody], HRP goat anti–mouse λ, HRP goat anti–mouse κ, and HRP goat anti–mouse IgG [γ chain–specific antibody]; SouthernBiotech). Additional primers used for generating probes are detailed in the Supplemental materials and methods (available at http://www.jem.org/cgi/content/full/jem.20082271/DC1).

Phage and PCR cloning. Tumor DNA samples were digested to completion with EcoRI, and fragments were cloned into either λZAP II vector (Stratagene) or λDASH II vector (Stratagene) according to the size of the fragments. Libraries were screened according to standard protocols (Stratagene) using Cλ1 or Jλ2 probe for λ rearrangements or translocations; *c-myc* probe A or *c-myc* probe D for *c-myc* translocations; Cα, Cγ1, and Sγ1 probes for S region rearrangement and translocations (see details for probes in the Supplemental materials and methods). Single plaques were purified, subcloned, and sequenced. In the case of λZAPII clones, the inserts were excised according to the protocol provided (Stratagene). Positive clones were verified by restriction analysis and hybridization. Sequencing of subcloned inserts was performed using T7 or T3 primers (DF-HCC DNA Resource Core). To obtain junctional sequences, internal primers were required for some tumors. For PCR cloning of Igλ rearrangements: Vlambda1int:5′-ttgtgactcaggaatctgca-3′ and Lamin 5′-ggagcagtctgaaatgagacaaagcat-3′ were used. Additional primers used for PCR cloning of junctions are detailed in Online supplemental material.

SKY and FISH analyses. Preparation of metaphase chromosomes, SKY analyses, FISH, and whole-chromosome painting using single-chromosome–specific paints were performed as previously described (61). FISH probes were as follows: a BAC that covered the 3′ region of the *IgH* locus encompassing *3′ IgH* enhancer and 100 kb downstream (3′ IgH BAC), a BAC just upstream of the *IgH* V_H region (5′ IgH BAC) as described previously (62), and a BAC that contained the *c-myc* gene (RP23-307D14, *c-myc* BAC). BACs for Igλ regions are RP23-382P9, RP23-60E14, RP23-374P12, and BACs for Igκ regions are RP23-84F6 and RP23-64I9. All the BACs were obtained from BACPAC CHORI database, except for the IgH BACs.

Online supplemental material. Fig. S1 shows the FACS, Northern blot, and RT-PCR data for assays used to characterize indicated surface protein and transcript expression by CXP lymphomas. Fig. S2 shows a Kaplan-Meier curve and summary of tumors that develop in $CX^{c/-}P^{c/c}$ lymphomas. Fig. S3 shows the evidence for specific *Xrcc4* deletion via CD21cre. Fig. S4 shows assays for *IgH* S region rearrangements in CXP lymphomas. Fig. S5 shows Southern blot data for Igκ and Igλ rearrangements and sequences of aberrant VλJλ joins in CXP lymphomas. Fig. S6 shows various characterizations of translocations in CXP tumors, including representative cytogenetic data (SKY, FISH, and chromosome paints) for analyses that were used to characterize *Igh/c-myc* translocations, Southern blots for characterization of *c-myc* rearrangements, Northern blot assays for *c-myc* expression, and sequences of translocation breakpoints. Fig. S7 displays cytogenetic data (SKY, FISH, and chromosome paints) for *Igλ* translocations, and sequence data for translocation breakpoints from CXP lymphomas. Fig. S8 displays CGH array data for analysis of genetic amplifications and deletions in CXP lymphomas. Table S1 summarizes the phenotypes of CXP lymphomas. Table S2 summarizes the phenotypes of $CX^{c/-}P^{c/c}$ lymphomas. Table S3 summarizes the characterized clonal translocations in CXP lympomas. Table S4 summarizes the characterized clonal translocations in $CX^{c/-}P^{c/c}$ lymphomas. The online supplemental material is available at http://www.jem.org/cgi/content/full/jem.20082271/DC1.

We thank Drs. L. Chin and Y. Xiao (The Belfer Cancer Genomics Center at Dana Farber Cancer Institute, Boston MA) for analysis of CGH data; Dr. S. Casola, P. Goff, and T. Hickernell for technical assistance and suggestions; Drs. J. Kutok and J. Aster (Brigham and Women's Hospital, Boston, MA) for histology analysis; and members of the Alt laboratory for discussions.

This work was supported by National Institutes of Health (NIH) grants 5P01 CA92625 (to F.W. Alt and K. Rajewsky), an NIH postdoctoral training grant NRSA T32 CA7008 (to C.T. Yan), Leukemia and Lymphoma Society (LLS) senior fellowships (to J.H. Wang and M. Gostissa), a LLS fellowship (to A. Datta). F.W. Alt is an investigator for the Howard Hughes Medical Institute.

The authors have no conflicting financial interests.

Submitted: 10 October 2008
Accepted: 18 November 2008

REFERENCES

1. Jung, D., C. Giallourakis, R. Mostoslavsky, and F.W. Alt. 2006. Mechanism and control of V(D)J recombination at the immunoglobulin heavy chain locus. *Annu. Rev. Immunol.* 24:541–570.
2. Jung, D., and F.W. Alt. 2004. Unraveling V(D)J recombination; insights into gene regulation. *Cell.* 116:299–311.
3. Rooney, S., J. Chaudhuri, and F.W. Alt. 2004. The role of the non-homologous end-joining pathway in lymphocyte development. *Immunol. Rev.* 200:115–131.
4. Li, Z., T. Otevrel, Y. Gao, H.L. Cheng, B. Seed, T.D. Stamato, G.E. Taccioli, and F.W. Alt. 1995. The XRCC4 gene encodes a novel protein involved in DNA double-strand break repair and V(D)J recombination. *Cell.* 83:1079–1089.
5. Grawunder, U., D. Zimmer, P. Kulesza, and M.R. Lieber. 1998. Requirement for an interaction of XRCC4 with DNA ligase IV for wild-type V(D)J recombination and DNA double-strand break repair in vivo. *J. Biol. Chem.* 273:24708–24714.
6. Gao, Y., Y. Sun, K.M. Frank, P. Dikkes, Y. Fujiwara, K.J. Seidl, J.M. Sekiguchi, G.A. Rathbun, W. Swat, J. Wang, et al. 1998. A critical role for DNA end-joining proteins in both lymphogenesis and neurogenesis. *Cell.* 95:891–902.
7. Frank, K.M., J.M. Sekiguchi, K.J. Seidl, W. Swat, G.A. Rathbun, H.L. Cheng, L. Davidson, L. Kangaloo, and F.W. Alt. 1998. Late embryonic lethality and impaired V(D)J recombination in mice lacking DNA ligase IV. *Nature.* 396:173–177.
8. Bassing, C.H., W. Swat, and F.W. Alt. 2002. The mechanism and regulation of chromosomal V(D)J recombination. *Cell.* 109(Suppl):S45–S55.
9. Gorman, J.R., and F.W. Alt. 1998. Regulation of immunoglobulin light chain isotype expression. *Adv. Immunol.* 69:113–181.
10. Schlissel, M.S. 2004. Regulation of activation and recombination of the murine Igkappa locus. *Immunol. Rev.* 200:215–223.
11. Vela, J.L., D. Ait-Azzouzene, B.H. Duong, T. Ota, and D. Nemazee. 2008. Rearrangement of mouse immunoglobulin kappa deleting element recombining sequence promotes immune tolerance and lambda B cell production. *Immunity.* 28:161–170.
12. Gay, D., T. Saunders, S. Camper, and M. Weigert. 1993. Receptor editing: an approach by autoreactive B cells to escape tolerance. *J. Exp. Med.* 177:999–1008.
13. Radic, M.Z., J. Erikson, S. Litwin, and M. Weigert. 1993. B lymphocytes may escape tolerance by revising their antigen receptors. *J. Exp. Med.* 177:1165–1173.
14. Tiegs, S.L., D.M. Russell, and D. Nemazee. 1993. Receptor editing in self-reactive bone marrow B cells. *J. Exp. Med.* 177:1009–1020.
15. Pelanda, R., S. Schwers, E. Sonoda, R.M. Torres, D. Nemazee, and K. Rajewsky. 1997. Receptor editing in a transgenic mouse model: site, efficiency, and role in B cell tolerance and antibody diversification. *Immunity.* 7:765–775.
16. Nemazee, D. 2006. Receptor editing in lymphocyte development and central tolerance. *Nat. Rev. Immunol.* 6:728–740.
17. Han, S., B. Zheng, D.G. Schatz, E. Spanopoulou, and G. Kelsoe. 1996. Neoteny in lymphocytes: Rag1 and Rag2 expression in germinal center B cells. *Science.* 274:2094–2097.
18. Han, S., S.R. Dillon, B. Zheng, M. Shimoda, M.S. Schlissel, and G. Kelsoe. 1997. V(D)J recombinase activity in a subset of germinal center B lymphocytes. *Science.* 278:301–305.
19. Hikida, M., M. Mori, T. Takai, K. Tomochika, K. Hamatani, and H. Ohmori. 1996. Reexpression of RAG-1 and RAG-2 genes in activated mature mouse B cells. *Science.* 274:2092–2094.
20. Papavasiliou, F., R. Casellas, H. Suh, X.F. Qin, E. Besmer, R. Pelanda, D. Nemazee, K. Rajewsky, and M.C. Nussenzweig. 1997. V(D)J recombination in mature B cells: a mechanism for altering antibody responses. *Science.* 278:298–301.
21. Hertz, M., V. Kouskoff, T. Nakamura, and D. Nemazee. 1998. V(D)J recombinase induction in splenic B lymphocytes is inhibited by antigen-receptor signalling. *Nature.* 394:292–295.
22. Gartner, F., F.W. Alt, R.J. Monroe, and K.J. Seidl. 2000. Antigen-independent appearance of recombination activating gene (RAG)–positive bone marrow B cells in the spleens of immunized mice. *J. Exp. Med.* 192:1745–1754.
23. Nagaoka, H., G. Gonzalez-Aseguinolaza, M. Tsuji, and M.C. Nussenzweig. 2000. Immunization and infection change the number of recombination activating gene (RAG)–expressing B cells in the periphery by altering immature lymphocyte production. *J. Exp. Med.* 191:2113–2120.
24. Monroe, R.J., K.J. Seidl, F. Gaertner, S. Han, F. Chen, J. Sekiguchi, J. Wang, R. Ferrini, L. Davidson, G. Kelsoe, and F.W. Alt. 1999. RAG2:GFP knockin mice reveal novel aspects of RAG2 expression in primary and peripheral lymphoid tissues. *Immunity.* 11:201–212.
25. Yu, W., H. Nagaoka, M. Jankovic, Z. Misulovin, H. Suh, A. Rolink, F. Melchers, E. Meffre, and M.C. Nussenzweig. 1999. Continued RAG expression in late stages of B cell development and no apparent re-induction after immunization. *Nature.* 400:682–687.
26. Igarashi, H., N. Kuwata, K. Kiyota, K. Sumita, T. Suda, S. Ono, S.R. Bauer, and N. Sakaguchi. 2001. Localization of recombination activating gene 1/green fluorescent protein (RAG1/GFP) expression in secondary lymphoid organs after immunization with T-dependent antigens in rag1/gfp knockin mice. *Blood.* 97:2680–2687.
27. Chaudhuri, J., U. Basu, A. Zarrin, C. Yan, S. Franco, T. Perlot, B. Vuong, J. Wang, R.T. Phan, A. Datta, et al. 2007. Evolution of the immunoglobulin heavy chain class switch recombination mechanism. *Adv. Immunol.* 94:157–214.
28. Muramatsu, M., K. Kinoshita, S. Fagarasan, S. Yamada, Y. Shinkai, and T. Honjo. 2000. Class switch recombination and hypermutation require activation-induced cytidine deaminase (AID), a potential RNA editing enzyme. *Cell.* 102:553–563.
29. Di Noia, J.M., and M.S. Neuberger. 2007. Molecular mechanisms of antibody somatic hypermutation. *Annu. Rev. Biochem.* 76:1–22.
30. Yan, C.T., C. Boboila, E.K. Souza, S. Franco, T.R. Hickernell, M. Murphy, S. Gumaste, M. Geyer, A.A. Zarrin, J.P. Manis, et al. 2007.

IgH class switching and translocations use a robust non-classical end-joining pathway. *Nature*. 449:478–482.
31. Gao, Y., D.O. Ferguson, W. Xie, J.P. Manis, J. Sekiguchi, K.M. Frank, J. Chaudhuri, J. Horner, R.A. DePinho, and F.W. Alt. 2000. Interplay of p53 and DNA-repair protein XRCC4 in tumorigenesis, genomic stability and development. *Nature*. 404:897–900.
32. Vogelstein, B., D. Lane, and A.J. Levine. 2000. Surfing the p53 network. *Nature*. 408:307–310.
33. Mills, K.D., D.O. Ferguson, and F.W. Alt. 2003. The role of DNA breaks in genomic instability and tumorigenesis. *Immunol. Rev.* 194:77–95.
34. Zhu, C., K.D. Mills, D.O. Ferguson, C. Lee, J. Manis, J. Fleming, Y. Gao, C.C. Morton, and F.W. Alt. 2002. Unrepaired DNA breaks in p53-deficient cells lead to oncogenic gene amplification subsequent to translocations. *Cell*. 109:811–821.
35. Kuppers, R., and R. Dalla-Favera. 2001. Mechanisms of chromosomal translocations in B cell lymphomas. *Oncogene*. 20:5580–5594.
36. Takahashi, K., Y. Kozono, T.J. Waldschmidt, D. Berthiaume, R.J. Quigg, A. Baron, and V.M. Holers. 1997. Mouse complement receptors type 1 (CR1;CD35) and type 2 (CR2;CD21): expression on normal B cell subpopulations and decreased levels during the development of autoimmunity in MRL/lpr mice. *J. Immunol.* 159:1557–1569.
37. Kraus, M., M.B. Alimzhanov, N. Rajewsky, and K. Rajewsky. 2004. Survival of resting mature B lymphocytes depends on BCR signaling via the Igalpha/beta heterodimer. *Cell*. 117:787–800.
38. Mostoslavsky, R., F.W. Alt, and K. Rajewsky. 2004. The lingering enigma of the allelic exclusion mechanism. *Cell*. 118:539–544.
39. Retter, M.W., and D. Nemazee. 1998. Receptor editing occurs frequently during normal B cell development. *J. Exp. Med.* 188:1231–1238.
40. Boudinot, P., A.M. Drapier, P.A. Cazenave, and P. Sanchez. 1994. Mechanistic and selective constraints act on the establishment of V lambda J lambda junctions in the B cell repertoire. *J. Immunol.* 152:2248–2255.
41. Malynn, B.A., T.K. Blackwell, G.M. Fulop, G.A. Rathbun, A.J. Furley, P. Ferrier, L.B. Heinke, R.A. Phillips, G.D. Yancopoulos, and F.W. Alt. 1988. The scid defect affects the final step of the immunoglobulin VDJ recombinase mechanism. *Cell*. 54:453–460.
42. Rooney, S., J. Sekiguchi, S. Whitlow, M. Eckersdorff, J.P. Manis, C. Lee, D.O. Ferguson, and F.W. Alt. 2004. Artemis and p53 cooperate to suppress oncogenic N-myc amplification in progenitor B cells. *Proc. Natl. Acad. Sci. USA*. 101:2410–2415.
43. Nilsson, J.A., and J.L. Cleveland. 2003. Myc pathways provoking cell suicide and cancer. *Oncogene*. 22:9007–9021.
44. Hemann, M.T., A. Bric, J. Teruya-Feldstein, A. Herbst, J.A. Nilsson, C. Cordon-Cardo, J.L. Cleveland, W.P. Tansey, and S.W. Lowe. 2005. Evasion of the p53 tumour surveillance network by tumour-derived MYC mutants. *Nature*. 436:807–811.
45. Ramiro, A.R., M. Jankovic, T. Eisenreich, S. Difilippantonio, S. Chen-Kiang, M. Muramatsu, T. Honjo, A. Nussenzweig, and M.C. Nussenzweig. 2004. AID is required for c-myc/IgH chromosome translocations in vivo. *Cell*. 118:431–438.
46. Kovalchuk, A.L., W. duBois, E. Mushinski, N.E. McNeil, C. Hirt, C.F. Qi, Z. Li, S. Janz, T. Honjo, M. Muramatsu, et al. 2007. AID-deficient Bcl-xL transgenic mice develop delayed atypical plasma cell tumors with unusual Ig/Myc chromosomal rearrangements. *J. Exp. Med*. 204:2989–3001.
47. Boxer, L.M., and C.V. Dang. 2001. Translocations involving c-myc and c-myc function. *Oncogene*. 20:5595–5610.
48. Kaye, J.A., J.A. Melo, S.K. Cheung, M.B. Vaze, J.E. Haber, and D.P. Toczyski. 2004. DNA breaks promote genomic instability by impeding proper chromosome segregation. *Curr. Biol.* 14:2096–2106.
49. Nadel, B., P.A. Cazenave, and P. Sanchez. 1990. Murine lambda gene rearrangements: the stochastic model prevails over the ordered model. *EMBO J.* 9:435–440.
50. Mao, C., L. Jiang, M. Melo-Jorge, M. Puthenveetil, X. Zhang, M.C. Carroll, and T. Imanishi-Kari. 2004. T cell-independent somatic hypermutation in murine B cells with an immature phenotype. *Immunity*. 20:133–144.
51. Crouch, E.E., Z. Li, M. Takizawa, S. Fichtner-Feigl, P. Gourzi, C. Montano, L. Feigenbaum, P. Wilson, S. Janz, F.N. Papavasiliou, and R. Casellas. 2007. Regulation of AID expression in the immune response. *J. Exp. Med*. 204:1145–1156.
52. Cascalho, M., A. Ma, S. Lee, L. Masat, and M. Wabl. 1996. A quasi-monoclonal mouse. *Science*. 272:1649–1652.
53. Callen, E., M. Jankovic, S. Difilippantonio, J.A. Daniel, H.T. Chen, A. Celeste, M. Pellegrini, K. McBride, D. Wangsa, A.L. Bredemeyer, et al. 2007. ATM prevents the persistence and propagation of chromosome breaks in lymphocytes. *Cell*. 130:63–75.
54. Difilippantonio, S., E. Gapud, N. Wong, C.Y. Huang, G. Mahowald, H.T. Chen, M.J. Kruhlak, E. Callen, F. Livak, M.C. Nussenzweig, B.P. Sleckman, and A. Nussenzweig. 2008. 53BP1 facilitates long-range DNA end-joining during V(D)J recombination. *Nature*.
55. MacLennan, I.C., K.M. Toellner, A.F. Cunningham, K. Serre, D.M. Sze, E. Zuniga, M.C. Cook, and C.G. Vinuesa. 2003. Extrafollicular antibody responses. *Immunol. Rev.* 194:8–18.
56. Donehower, L.A., M. Harvey, B.L. Slagle, M.J. McArthur, C.A. Montgomery Jr., J.S. Butel, and A. Bradley. 1992. Mice deficient for p53 are developmentally normal but susceptible to spontaneous tumours. *Nature*. 356:215–221.
57. Jonkers, J., R. Meuwissen, H. van der Gulden, H. Peterse, M. van der Valk, and A. Berns. 2001. Synergistic tumor suppressor activity of BRCA2 and p53 in a conditional mouse model for breast cancer. *Nat. Genet*. 29:418–425.
58. Frank, K.M., N.E. Sharpless, Y. Gao, J.M. Sekiguchi, D.O. Ferguson, C. Zhu, J.P. Manis, J. Horner, R.A. DePinho, and F.W. Alt. 2000. DNA ligase IV deficiency in mice leads to defective neurogenesis and embryonic lethality via the p53 pathway. *Mol. Cell*. 5:993–1002.
59. Van Ness, B.G., M. Weigert, C. Coleclough, E.L. Mather, D.E. Kelley, and R.P. Perry. 1981. Transcription of the unrearranged mouse C kappa locus: sequence of the initiation region and comparison of activity with a rearranged V kappa-C kappa gene. *Cell*. 27:593–602.
60. Moore, M.W., J. Durdik, D.M. Persiani, and E. Selsing. 1985. Deletions of kappa chain constant region genes in mouse lambda chain-producing B cells involve intrachromosomal DNA recombinations similar to V-J joining. *Proc. Natl. Acad. Sci. USA*. 82:6211–6215.
61. Sharpless, N.E., D.O. Ferguson, R.C. O'Hagan, D.H. Castrillon, C. Lee, P.A. Farazi, S. Alson, J. Fleming, C.C. Morton, K. Frank, et al. 2001. Impaired nonhomologous end-joining provokes soft tissue sarcomas harboring chromosomal translocations, amplifications, and deletions. *Mol. Cell*. 8:1187–1196.
62. Franco, S., M. Gostissa, S. Zha, D.B. Lombard, M.M. Murphy, A.A. Zarrin, C. Yan, S. Tepsuporn, J.C. Morales, M.M. Adams, et al. 2006. H2AX prevents DNA breaks from progressing to chromosome breaks and translocations. *Mol. Cell*. 21:201–214.